Lee Model

Hunt Feng[1]

[1]Department of Physics and Engineering Physics
University of Saskatchewan

November 27, 2023

Outline of Presentation

1. Review of DPF
2. Simulation

Outline of Presentation

1. Review of DPF
2. Simulation

Different Phases in DPF

- Three phases: break down, axial, and compression phases.
- Compression phase: inward shockwave, reflected shockwave, and slow compression phase.

Break Down Phase

- Gas is ionized, and current layer formed

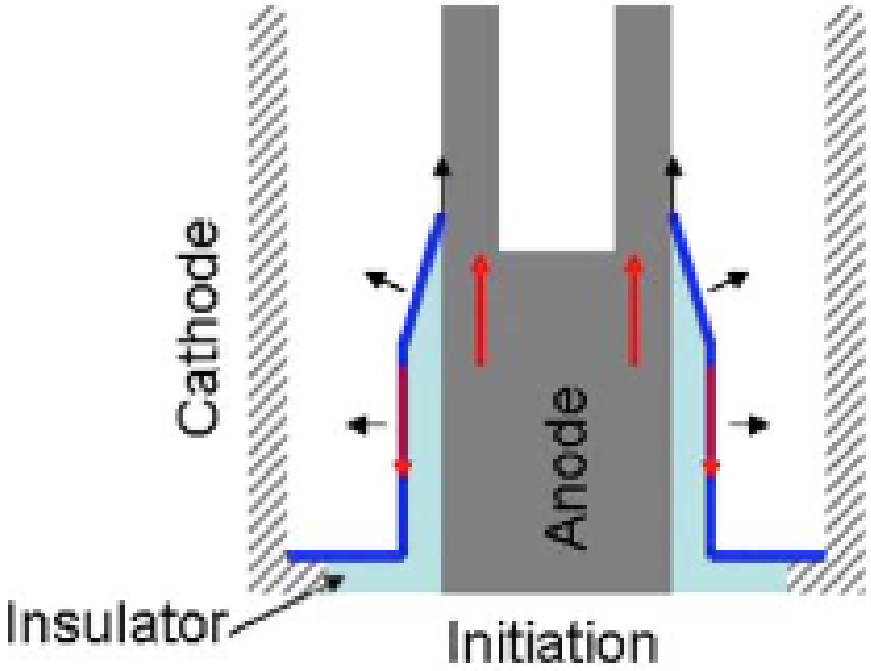

Figure 1: Initiation via flashover of the insulator. Break down phase. [5]

Axial Phase

- Current layer is accelerated by the $\mathbf{J} \times \mathbf{B}$ force in the axial direction.
- A shockwave (SW) is formed due to magnetic pressure (MP).

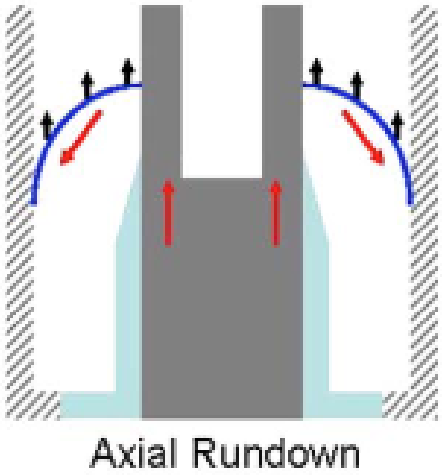

(a) Axial run-down phase. [5]

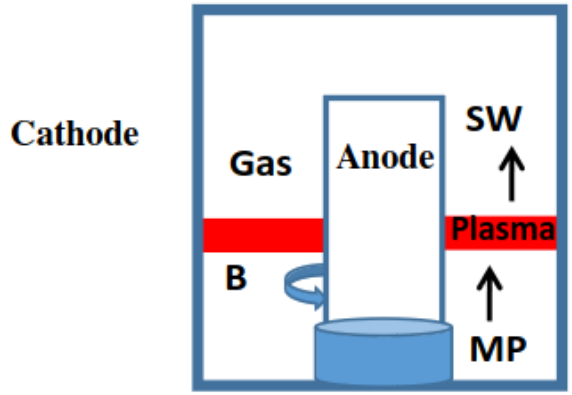

(b) The formation of plasma layer. [3]

Compression Phase - Inward Shockwave Phase

- When the plasma layer arrives at the top of the anode, the $\mathbf{J} \times \mathbf{B}$ force pushes them into the center of the anode.
- Plasma column with inner radius r_s and outer radius r_p will form on the top of the anode.
- Shockwave compresses gas in the center.

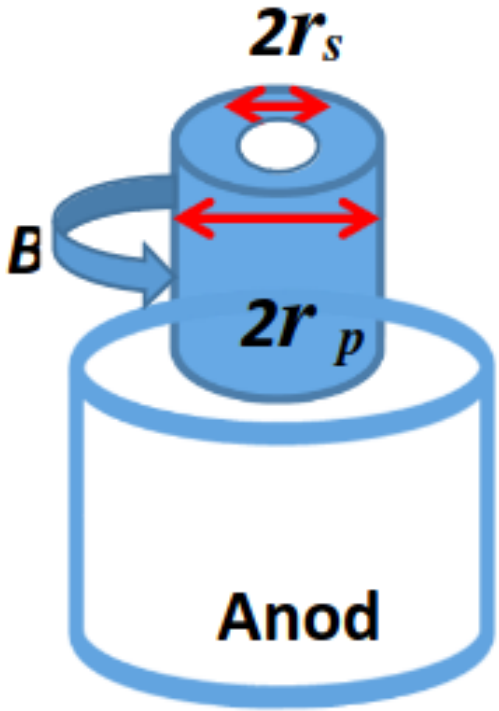

Figure 3: The inward radial shock wave in final stage off plasma focus.

Compression Phase - Reflected Shockwave Phase

- The shockwave will be reflected radially in the outward direction after hitting the center of the anode.

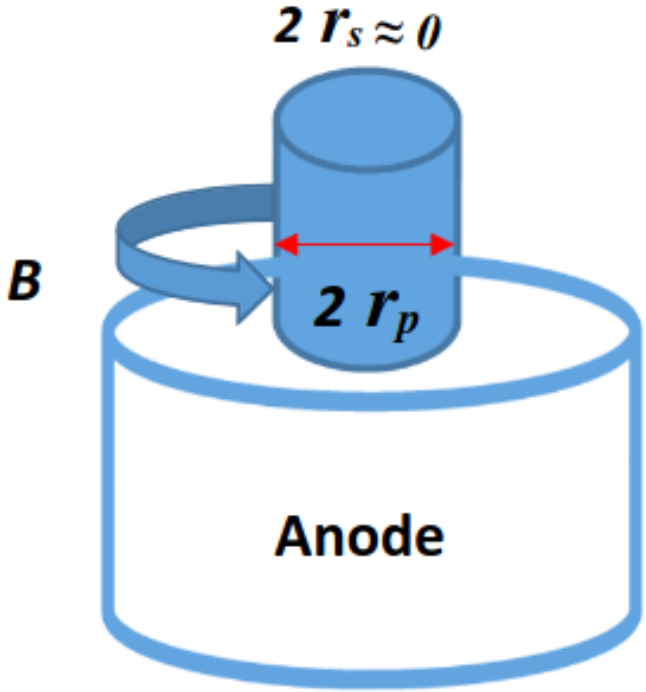

Figure 4: The reflected shockwave phase in plasma focus. [3]

Compression Phase - Slow Compression Phase

- Slow compression phase starts when $r_s = r_p$.
- The reflected shockwave produces a pressure in the opposite direction of the magnetic pressure.
- Plasma column will be compressed to its minimum radius.

Instability Phase

- When plasma reaches maximum compression, the plasma column may become unstable due to plasma instabilities.
- Instabilities make the plasma resistance anomalous.

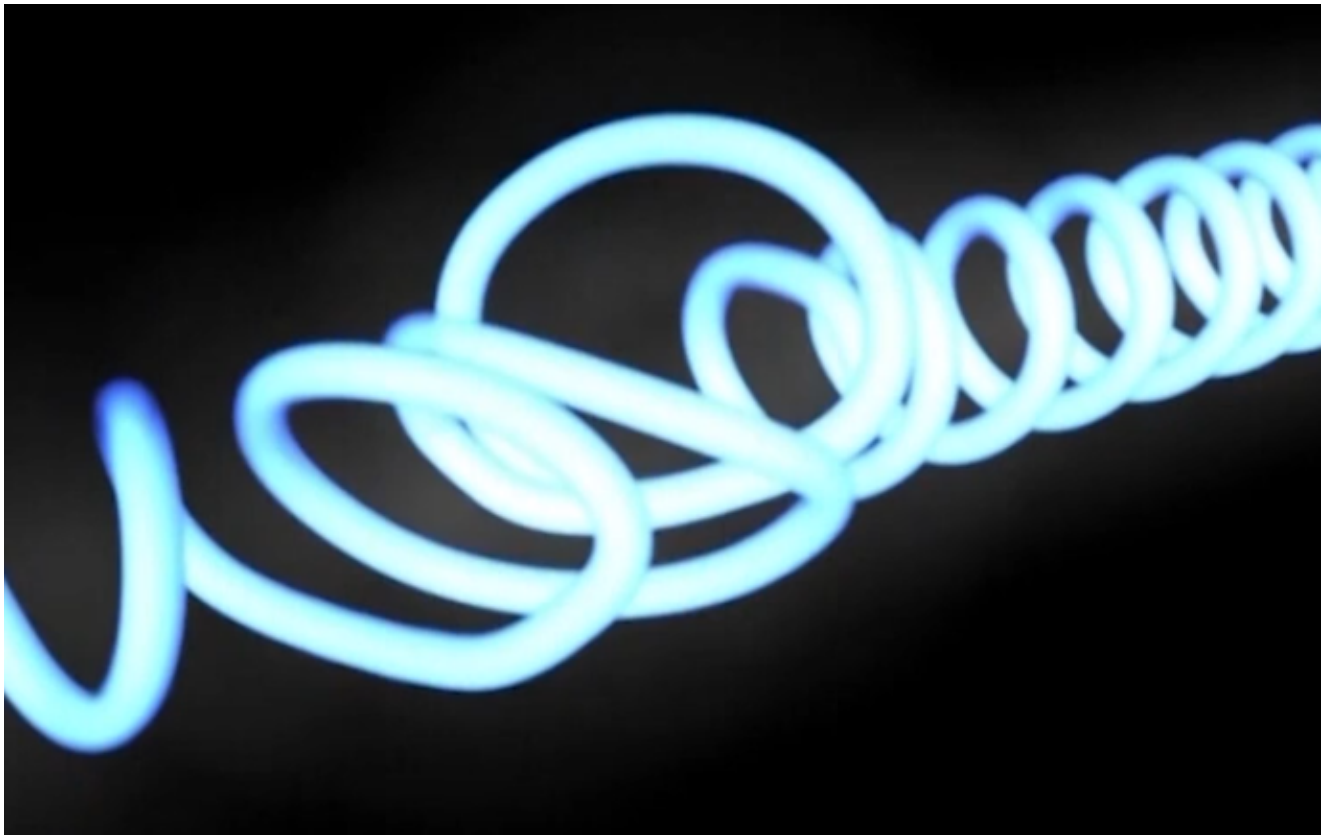

Figure 5: Plasma column is twisted in instability phase. Source [2]

Outline of Presentation

1 Review of DPF

2 Simulation

Parameters

L_0 (nH)	C_0 (mF)	b (cm)	a (cm)	z_0 (cm)	r_0 (mW)
20	28	4.1	1.9	5	2.3
f_m	f_c	f_{mr}	f_{cr}	Model Parameters	
0.0635	0.7	0.16	0.7		
V_0 (kV)	P_0 (Torr)	Molecular W	Atomic Nur	At=1, Mol=2	Operational
11	2.63	20	10	1	Parameters

Figure 6: Input Parameters

- The parameters are set to match the device NX2.
- Bank parameters, L_0, C_0 and stray circuit resistance r_0.
- Tube parameters b, a and z_0.
- Operational parameters V_0 and P_0 and the fill gas.

Parameters - Continue

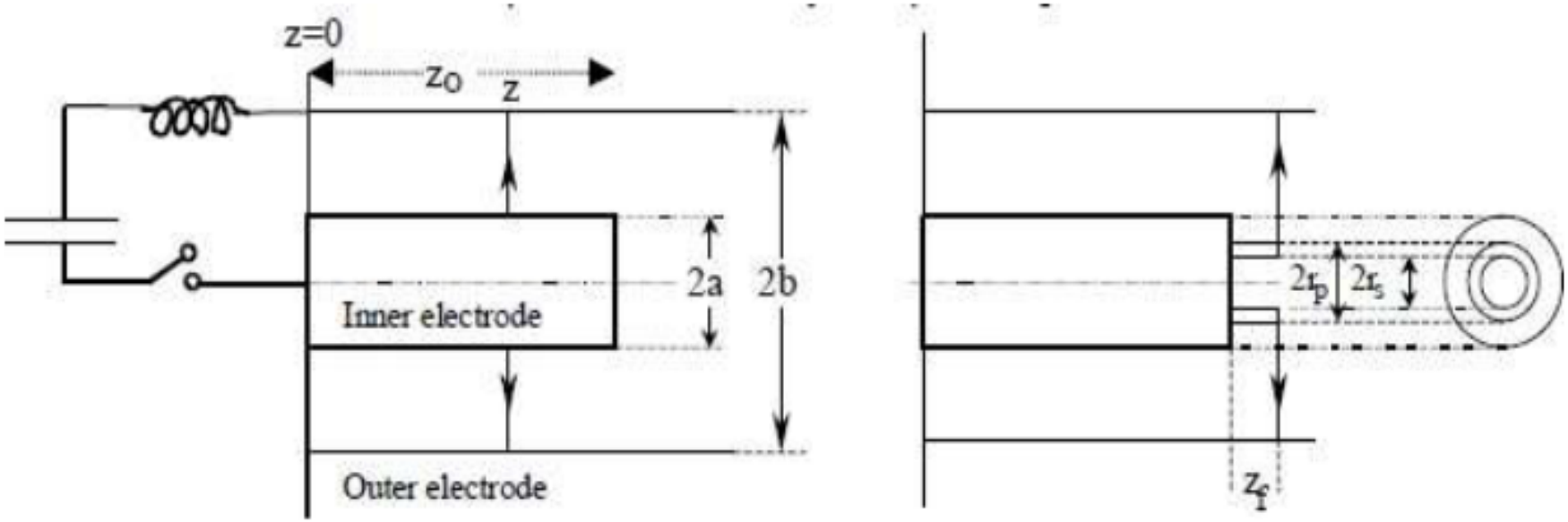

Figure 7: DPF device.

Discharge Current

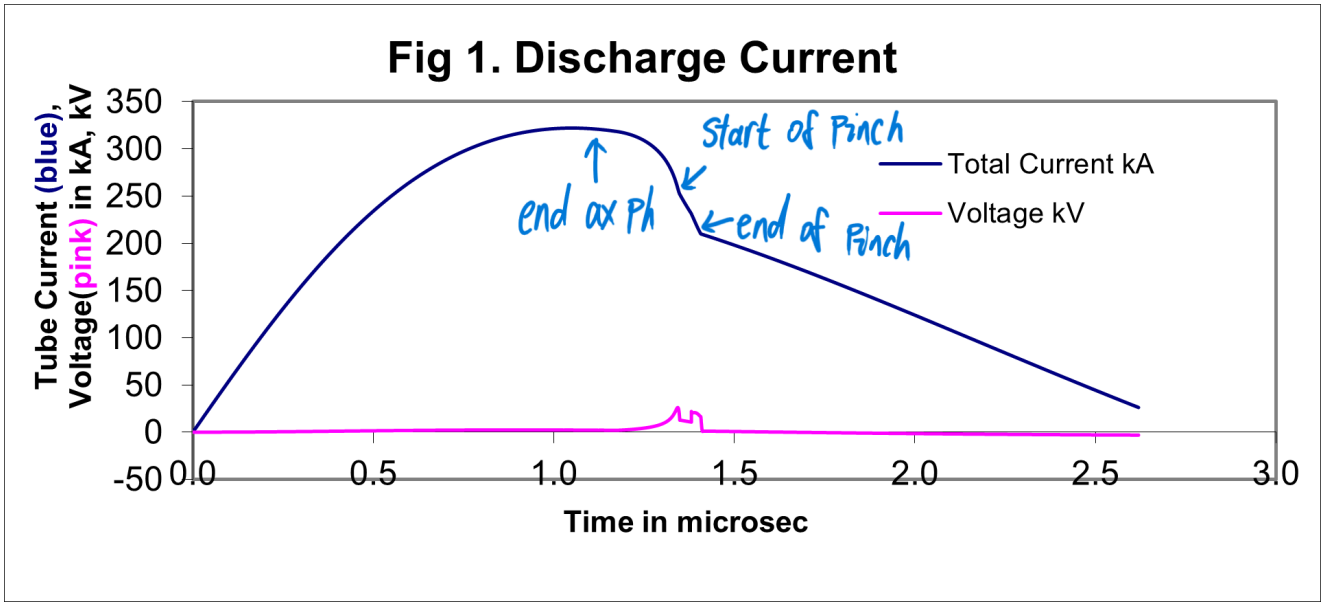

Figure 8: Discharge Current

- Axial phase ends after the discharge current reaches its peak (1.17μs).
- As the radial phase starts, the discharge current decreases.
- The pinch starts at 1.38μs.
- Then at 1.41μs the radial phase ends, also the pinch ends.

5-Point Fitting

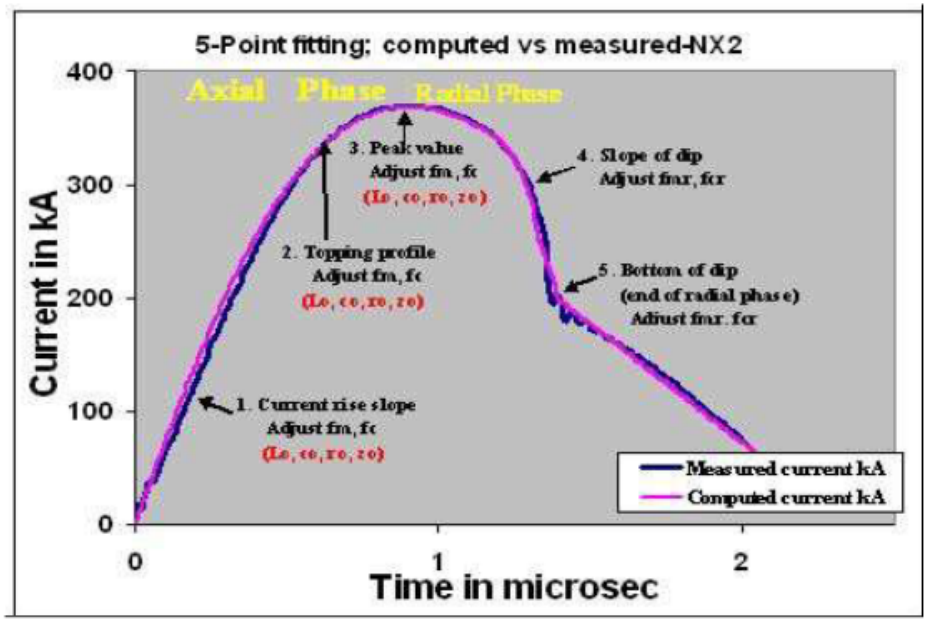

Figure 9: The 5-point fitting of computed current trace to measured (reference) current trace. Point 1 is the current rise slope. Point 2 is the topping profile. Point 3 is the peak value of the current. Point 4 is the slope of the current dip. Point 5 is the bottom of the current dip. Fitting is done up to point 5 only. Further agreement or divergence of the computed trace with/from the measured trace is only incidental and not considered to be important.

- By fitting the 5 features, we are able to obtained the fitted model parameters: f_m, f_c, f_{mr}, and f_{cr}.

Speed of Current Sheet

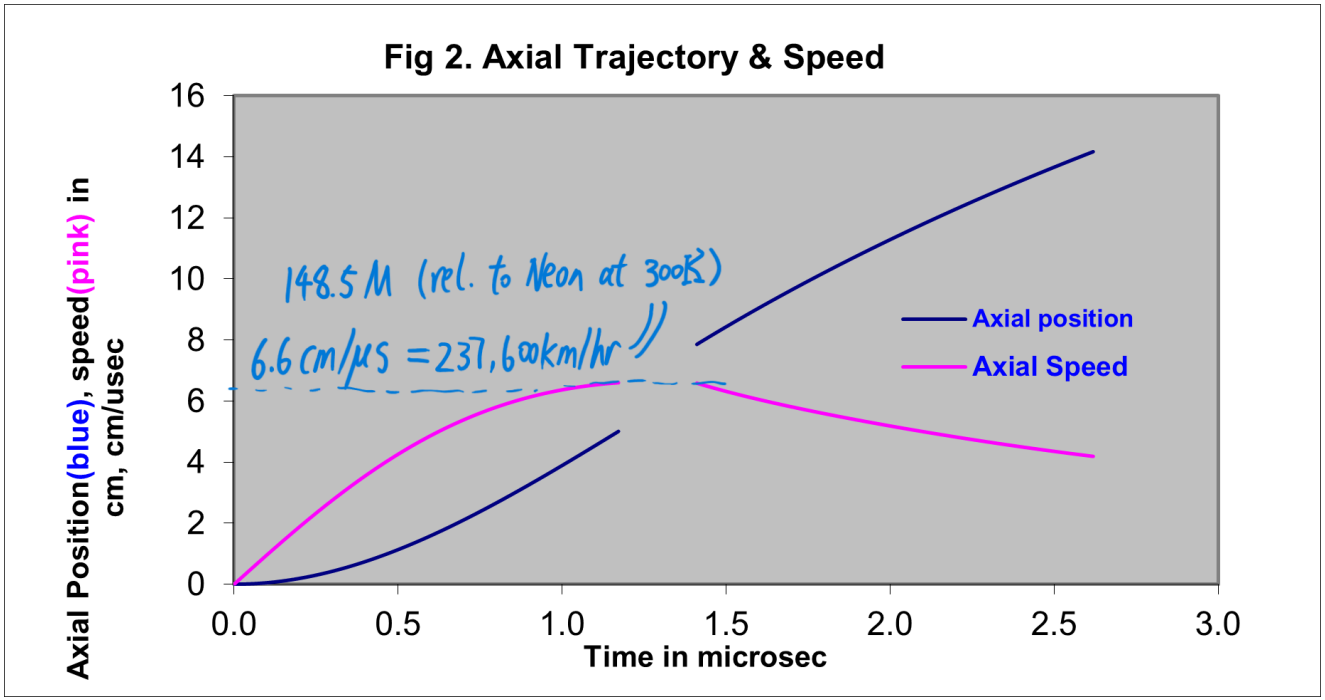

Figure 10: Axial Speed of the current sheet.

- The speed of current sheet is fast.
- The speed of sound of Neon is 1500km/h. The Mach number is therefore 150M.

Radial Position

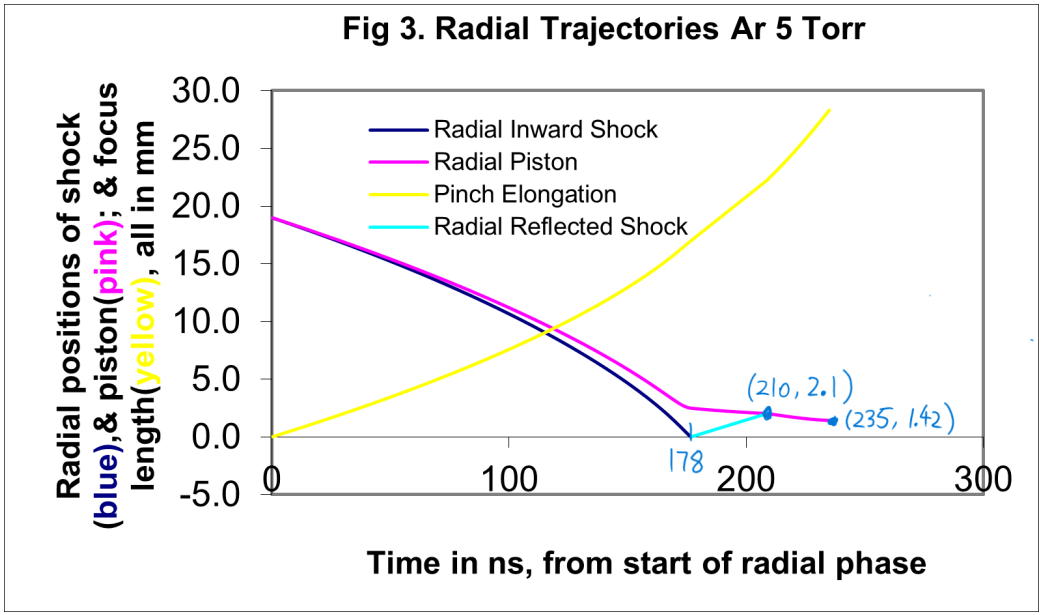

Figure 11: Radial position of the plasma column starting from radial phase.

- In the radial inward shock phase, both inner and outer radius of the plasma column decreases.
- After 178ns, radial reflected shock phase starts and the inner radius of the plasma column increases.
- After 210ns, it enters slow compression phase and the plasma column will be compressed to its minimum radius.

Temperature

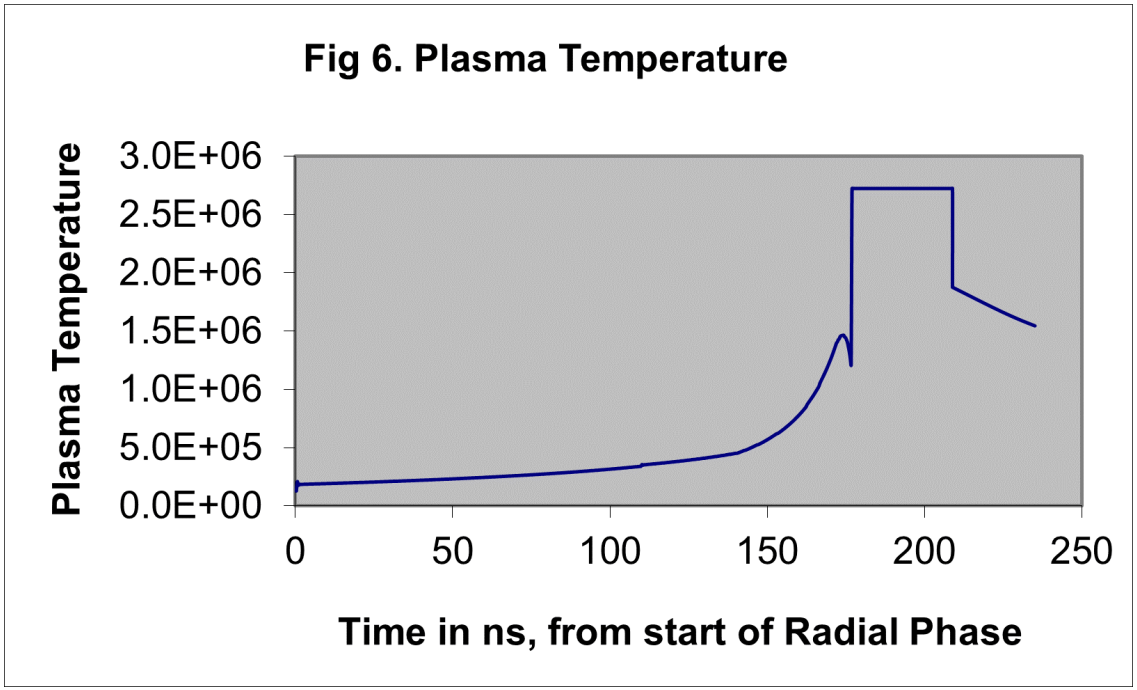

Figure 12: Plasma temperature in radial phase.

- The plasma temperature raises during the radial inward shock phase.
- The plasma temperature reaches its maximum 2.72×10^6K during the radial reflected shock phase.
- The temperature stays constant during the radial reflected shock phase.

Radiation

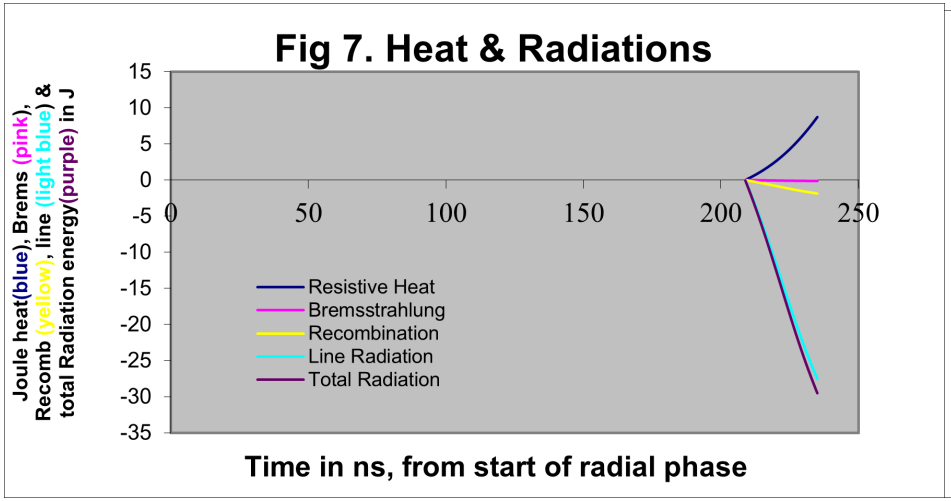

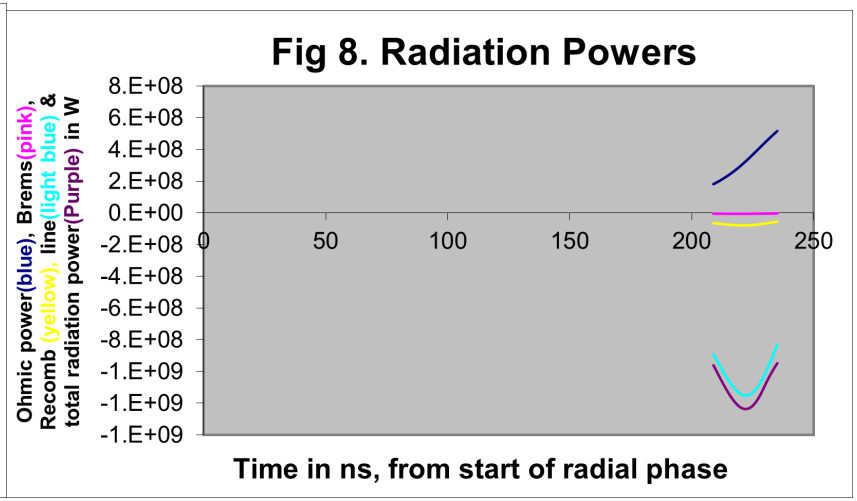

Figure 13: Radiation related graphs

- Radiations starts after the pinch ends (plasmoid) is formed.
- Joule heating reached a maximum value of 8.73J
- Total radiation reached a maximum value of 30J


Dense plasma focus — Plasma-Universe.com — plasma-universe.com.
https://www.plasma-universe.com/dense-plasma-focus/.
[Accessed 16-10-2023].


DPF Device - LPP Fusion — lppfusion.com.
https://www.lppfusion.com/technology/focus-fusion-energy/dpf-device/.
[Accessed 16-10-2023].


R. Behbahani.
Enhancement of Charged Particle Emission from a Plasma Focus Device.
Phd thesis, University of Saskatchewan, 2017.


V. A. Gribkov, I. V. Borovitskaya, E. V. Demina, E. E. Kazilin, S. V. Latyshev, S. A. Maslyaev, V. N. Pimenov, T. Laas, M. Paduch, and S. V. Rogozhkin.
Application of dense plasma focus devices and lasers in the radiation material sciences for the goals of inertial fusion beyond ignition.
Matter and Radiation at Extremes, 5(4):045403, 06 2020.


M. Krishnan.
The dense plasma focus: A versatile dense pinch for diverse applications.
IEEE transactions on plasma science, 40(12):3189–3221, 2012.


E. J. Lerner, S. M. Hassan, I. Karamitsos-Zivkovic, and R. Fritsch.
Focus Fusion: Overview of Progress Towards p-B11 Fusion with the Dense Plasma Focus.
Journal of Fusion Energy, 42(1), mar 9 2023.


R. S. Rawat.
Dense plasma focus - from alternative fusion source to versatile high energy density plasma source for plasma nanotechnology.
Journal of Physics: Conference Series, 591(1):012021, mar 2015.


P. Sharma, J. V. Vas, R. Medwal, M. Mishra, A. Chaurasiya, M. T. Luai, Z. Zheng, V. Chaudhary, R. V. Ramanujan, L. C. K. Paul, C. Xiao, and R. S. Rawat.
High energy density pulsed argon plasma synthesized nanostructured tungsten for damage mitigation under fusion relevant energetic he ion irradiation.
Applied Surface Science Advances, 6:100172, 2021.